



Single Event Latch-Up Characterization of the Radiation Assured Devices RAD1419 14-Bit, 800ksps Sampling A/D Converter with Shutdown

Customer: Radiation Assured Devices

RAD Job Number: 10-xxx

Part Type Tested/SMD: Radiation Assured Devices RAD1419 14-Bit, 800ksps Sampling A/D Converter with Shutdown

Traceability Information: Wafer Lot: W0945251-05, Wafer 3, Lot Date code: 1012; see Appendix A for a photograph of a sample unit-under-test.

Referenced Test Standard(s): ASTM F1192, EIA/JESD57

Electrical Test Conditions: During the beam run, the units were biased with a static split 5.5V potential on V_{DD} , DV_{DD} and V_{SS} . The memories were tested until a total fluence of $1E7\text{ion/cm}^2$ or until a latch-up event was detected. The supply current was monitored and recorded during exposure. See Appendix B for the details of the bias conditions.

Test Software / Hardware: ICC.XLS, See Appendix C, Table C.3 for a list of test equipment and calibration dates.

Ion Energy and LET Ranges: 10MeV/n Xe and Kr beams with effective LETs from $43\text{MeV-cm}^2/\text{mg}$ to $80\text{MeV-cm}^2/\text{mg}$. The 10MeV/n Xe beam had a minimum range of $50\mu\text{m}$ in silicon to the Bragg Peak.

Heavy Ion Flux and Maximum Fluence Levels: Flux of approximately $2\text{ions/cm}^2\text{-s}$ to $5E5\text{ions/cm}^2\text{-s}$. Minimum of $1E7\text{ions/cm}^2$ per unit tested or until a latch-up event was detected.

Facility and/or Radiation Source: Lawrence Berkeley National Laboratories (LBNL) Berkeley, CA (10MeV/n beam).

Irradiation Temperature: 85°C case temperature as specified as the typical high-temperature use condition.

The units-under-test did not exhibit latch-up at any LETs of $55\text{MeV-cm}^2/\text{mg}$ or lower. SEL events were recorded and characterized using LETs from $58\text{MeV-cm}^2/\text{mg}$ to $83\text{MeV-cm}^2/\text{mg}$. The SEL events were non-destructive and have a very low limiting cross-section of $<3E-06\text{cm}^2/\text{device}$. Therefore the RAD1419 14-Bit ADC has a “worst-case” geosynchronous SEL rate of $<8E-08$ events/device-day or an MTBF of 12.5-million days. An equivalent failure in time (FIT) rate is approximately 3 failures/billion device-hours



1.0. Overview and Background

It is well known that heavy ion exposure can cause single event effects that can lead to temporary and/or permanent damage in electronic devices. The events can occur through various mechanisms including single event latch-up (SEL), single event burnout (SEB) and single event gate rupture (SEGR). An SEL event occurs when a parasitic npnp feedback latch structure becomes biased into the on state due to a dense track of electron-hole pairs created along the heavy ion path in silicon. This latch-up is self-sustaining since there is a positive feedback path created and requires a power cycle to reset. A single event latch-up can non-destructive or destructive. A non-destructive SEL event occurs if the latch-up event is “self-limiting” while a destructive SEL event occurs if the current draw from the SEL event is sufficient to damage the junction and/or bond wire. The damage can become worse and/or becomes evident with increasing linear energy transfer (LET) and fluence. The two test standards most frequently used to govern this testing are ASTM F1192 and EIA/JESD57. Single event latch-up testing is usually performed at the maximum datasheet voltage and temperature to a total fluence of not less than $1E7\text{ion/cm}^2$.

2.0. Single Event Latch-Up Test Apparatus

The single event latch-up testing described in this final report was performed at the Lawrence Berkeley National Laboratories (LBNL) using the 88-Inch Cyclotron. The 88-Inch Cyclotron is operated by the University of California for the US Department of Energy (DOE) and is a K=140 sector-focused cyclotron with both light- and heavy-ion capabilities. Protons and other light-ions are available at high intensities (10-20 μA) up to maximum energies of 55 MeV (protons), 65 MeV (deuterons), 135 MeV (3He) and 140 MeV (4He). Most heavy ions through uranium can be accelerated to maximum energies, which vary with the mass and charge state.

For the SEL testing described in this final report the devices were placed in the Cave 4B vacuum chamber aligned with the heavy ion beam line. The test platter in the vacuum chamber has full x and y alignment capabilities along with 2-dimensional rotation, allowing for a variety of effective LETs for each ion. For SEE testing Lawrence Berkeley Laboratories provides the dosimetry via a local control computer running a Lab View based program. Each ion is calibrated just prior to use using five photomultiplier tubes (PMTs). Four of the five PMTS are used during the test to provide the beam statistics, while the center PMT is removed following calibration. Figure 2.1 shows an illustration of the LBL facility; including the location of Cave 4B, where the heavy ion SEE testing took place.

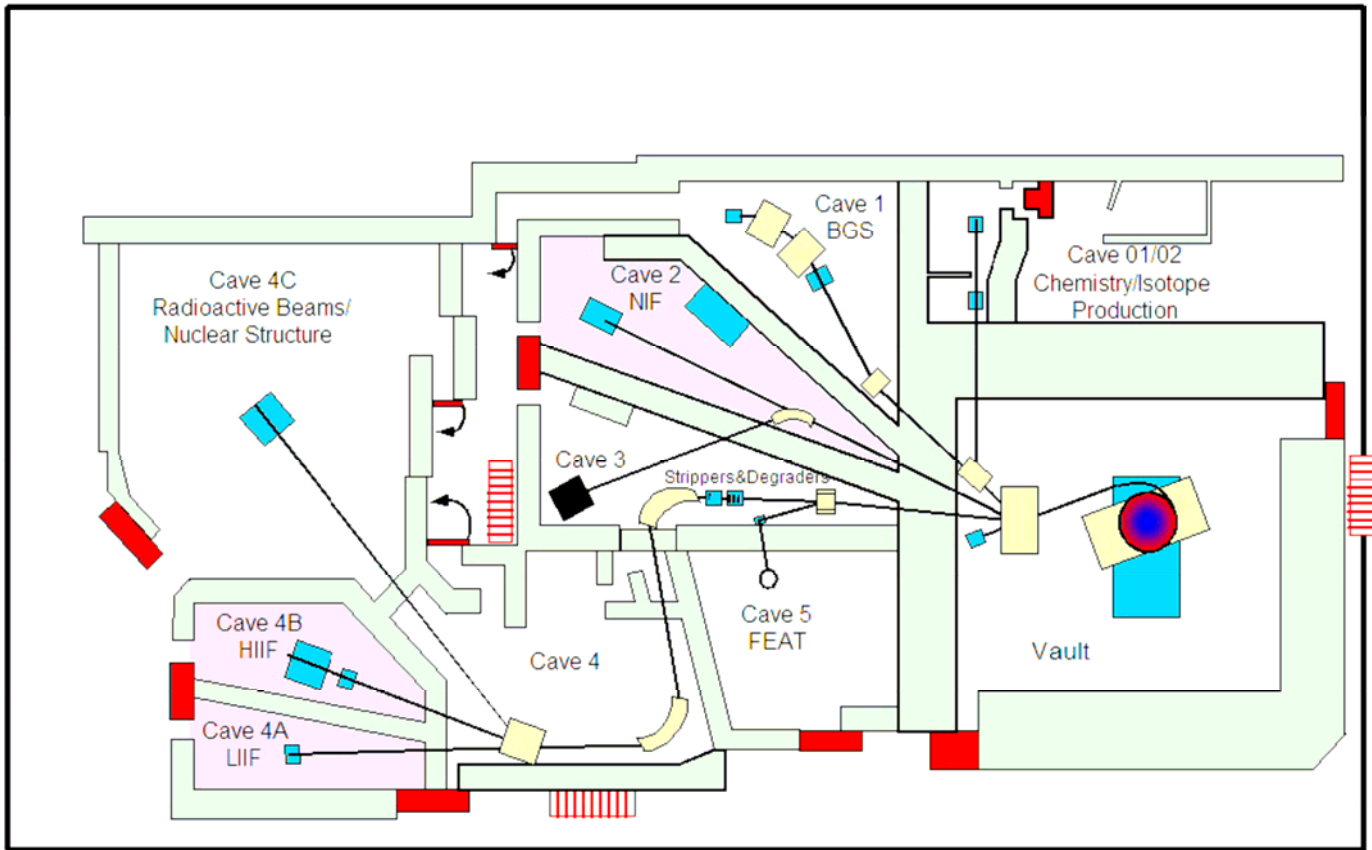


Figure 2.1. Map of 88-Inch Cyclotron Facility showing the location of Cave 4B, where the SEE testing was performed.



3.0. Radiation Test Conditions

The RAD1419 14-Bit, 800ksps Sampling A/D Converter with Shutdown described in this final report was irradiated using Kr and Xe with a split positive supply potential of 5.5V and at a maximum case temperature of 85°C. See the Bias Table in Appendix B for the specific details of the bias conditions. The 10MeV/n beam was used to provide sufficient range in silicon while meeting the maximum LET requirements of the program. The other beams available at Berkeley are the 4.5MeV/n beam and the 16MeV/n beam. The 4.5MeV/n beam does not provide sufficient range for destructive SEE testing while the 16MeV/n beam provides a much smaller selection of ions. Figure 3.1 shows the 10MeV/n beam characteristics for Xe. As seen in the figure, the range to the Bragg Peak is approximately 60µm while the surface LET is approximately 58MeV-cm²/mg. Note that the units were decapsulated prior to testing and all exposures took place from the top surface providing a distance to the active layer in Silicon of approximately 5 to 10µm. Figure 3.2 shows the characteristics for all the beams available at Berkeley.

The devices were irradiated to a minimum fluence of 1E7ion/cm² for each run or until a latch-up event was detected. The flux varied somewhat during the testing, but was consistently targeted to approximately to between 2E5ion/cm²-s and 5E5ion/cm²-s. As noted, the irradiation of the units-under-test continued until either the minimum fluence was reached or a latchup event was observed.

For the elevated temperature required for single event latch-up testing an aluminum plate heater fixed to the back of the board and was used to heat the device-under-test (DUT) with an RTD used to monitor the temperature. The case temperature of the DUT was calibrated prior to the testing to the RTD with a thermocouple, allowing the RTD to provide feedback and maintain a calibrated 85°C case temperature throughout the testing. The data monitored during the test (case temperature, supply voltage and supply current) was routed to the control room (approximately 20-feet away) using shielded coaxial cable.

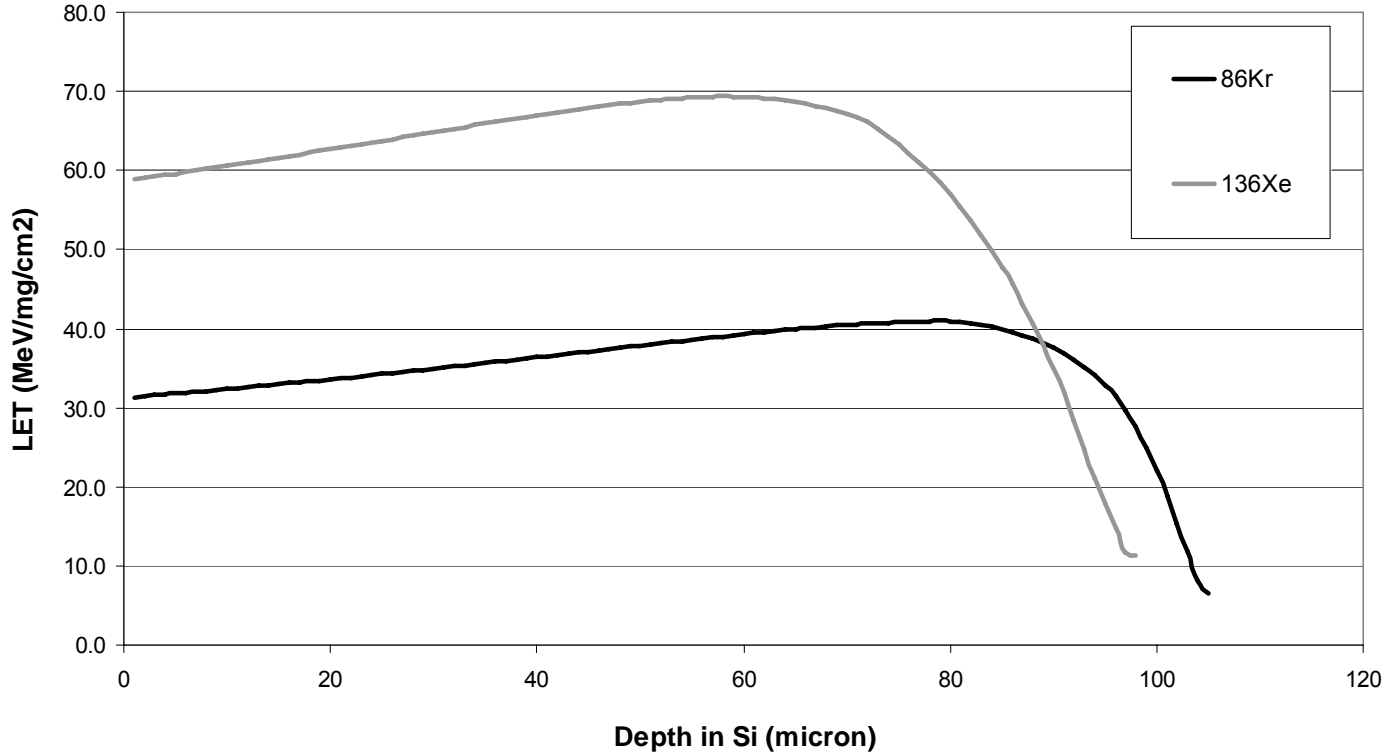


Figure 3.1. Range of the 10MeV/n Kr and Xe beam into silicon. The range to the Bragg Peak is approximately 80 μ m and 60 μ m while the surface LET is approximately 32MeV-cm²/mg and 58MeV-cm²/mg for Kr and Xe, respectively.



**SEL Characterization Report
10-xxx 100429 R1.0**

**Radiation Assured Devices
5017 N. 30th Street
Colorado Springs, CO 80919
(719) 531-0800**

Ion	Cocktail (MeV/nuc)	Energy (MeV)	Z	A	Chg. State	% Nat. Abund.	LET 0* (MeV/(mg/cm ²))	LET 60*	Range (μ m)	Method
B	4.5	44.90	5	10	+2	19.9	1.65	3.30	78.5	MIVOC
N	4.5	67.44	7	15	+3	0.37	3.08	6.16	67.8	Gas
Ne	4.5	89.95	10	20	+4	90.48	5.77	11.54	53.1	Gas
Si ¹	4.5	139.61	14	29	+6	4.67	9.28	18.56	52.4	Gas
Ar	4.5	180.00	18	40	+8	99.6	14.32	28.64	48.3	Gas
V	4.5	221.00	23	51	+10	99.75	21.68	43.36	42.5	Probe
Cu	4.5	301.79	29	63	+13	69.17	29.33	58.66	45.6	Probe
Kr	4.5	387.08	36	84	+17	17.3	36.96	77.92	48.0	Gas
Y	4.5	409.58	39	89	+18	100	45.58	91.16	45.8	Probe
Ag	4.5	499.50	47	109	+22	48.161	58.18	116.36	46.3	Probe
Xe	4.5	602.90	54	136	+27	8.9	68.84	137.68	48.3	Gas
Tb	4.5	724.17	65	159	+32	100	77.52	155.04	52.4	Probe
Ta	4.5	805.02	73	181	+36	99.988	87.15	174.30	53.0	Probe
Bi	4.5	904.16	83	209	+41	100	99.74	199.48	52.9	Oven
<hr/>										
B	10	108.01	5	11	+3	80.1	0.89	1.78	305.7	MIVOC
O	10	183.47	8	18	+5	0.2	2.19	4.38	226.4	Gas
Ne	10	216.28	10	22	+6	9.25	3.49	6.98	174.6	Gas
Si ¹	10	291.77	14	29	+8	4.67	6.09	12.18	141.7	Gas
Ar	10	400.00	18	40	+11	99.6	9.74	19.48	130.1	Gas
V	10	508.27	23	51	+14	99.75	14.59	29.18	113.4	Probe
Cu	10	659.19	29	65	+18	30.83	21.17	42.34	108.0	Probe
Kr	10	906.45	36	84	+24	57	30.23	60.46	113.1	Gas
Y	10	928.49	39	89	+25	100	34.73	69.46	102.2	Probe
Ag	10	1039.42	47	107	+29	51.839	48.15	96.30	90.0	Probe
Xe	10	1232.55	54	124	+34	0.1	58.78	117.56	90.0	Gas
<hr/>										
N	16	233.75	7	14	+5	99.63	1.16	2.32	505.9	Gas
O	16	277.33	8	17	+6	0.04	1.54	3.08	462.4	Gas
Ne	16	321.00	10	20	+7	90.48	2.39	4.78	347.9	Gas
Si ¹	16	452.10	14	29	+10	4.67	4.56	9.12	274.3	Gas
Cl	16	539.51	17	35	+12	75.77	6.61	13.22	233.6	Natural
Ar	16	642.36	18	40	+14	99.600	7.27	14.54	255.6	Gas
V	16	832.84	23	51	+18	99.750	10.90	21.80	225.8	Probe
Cu	16	1007.34	29	63	+22	69.17	16.53	33.06	190.3	Probe
Kr	16	1225.54	36	78	+27	0.35	24.98	49.96	165.4	Gas
Xe	16	1954.71	54	124	+43	0.1	49.29	98.58	147.9	Gas
<hr/>										
N	30	425.45	7	15	+7	0.37	0.76	1.52	1370.0	Gas
O	30	490.22	8	17	+8	0.04	0.98	1.96	1220.0	Gas
Ne	30	620.00	10	21	+10	0.27	1.48	2.96	1040.0	Gas
Ar	30	1046.11	18	36	+17	0.337	4.87	9.74	578.1	Gas

¹By Special request

Figure 3.2. Characteristics of all the beams available at Berkeley. For the testing discussed in this report the 10MeV/n beam was used exclusively, as discussed in the text.



4.0. Tested Parameters

During heavy ion exposure, the supply current to the unit-under-test was measured and recorded in approximately 1-second increments. A plot of supply current versus time/fluence for each of the heavy ion exposures is included in this final report. In addition to recording the supply current, the gross functionality of the device was monitored following the exposure and before power was cycled when the units under test did not latch-up. A full parametric test was also performed on all four SEL test units using the RAD1419 production test program approximately 3-days following the SEL testing.

In general the following two criteria must be met for a device to pass SEL testing: 1) SEL “immunity” to a minimum specified LET. This test is characterized by a heavy ion exposure to the minimum LET specified, typically $40\text{MeV}\cdot\text{cm}^2/\text{mg}$ to $80\text{MeV}\cdot\text{cm}^2/\text{mg}$ where the supply current must remain within the unit’s pre-exposure supply specification limits without cycling power, the unit-under-test must remain functional following the radiation exposure also without the need to cycle power. Finally, the SEL test units under test must pass a parametric test at some point following the SEL exposure to ensure no significant degradation occurred due to undetected events; or 2) SEL “characterization”. SEL characterization establishes the LET threshold and limiting cross-section, determines if the SEL events are destructive or non-destructive by verifying gross functionality immediately following a power cycle. These units also must pass a parametric test at some point following the SEL exposure to ensure no significant degradation occurred due to the detected or undetected SEL events. Once the characterization is complete the SEL threshold and cross-section data is used with a space radiation modeling code (such as CREME96) to determine if the SEL rate is acceptable for the mission application. If any of these conditions are not satisfied following the heavy ion testing, then the units (from the lot date code tested) could be logged as an SEL failure and may not be suitable for space flight application. Note that during heavy ion testing a substantial amount of total dose can be absorbed by the units-under-test. If a functional or parameter failure occurs during or following the SEL testing, it is important to separate TID failures from destructive single event effects.

5.0. Single Event Latch-Up Test Results

The RAD1419 14-Bit, 800ksps Sampling A/D Converter with Shutdown SEL test units-under-test did not exhibit latch-up at any LETs of $55\text{MeV}\cdot\text{cm}^2/\text{mg}$ or lower. SEL events were recorded and characterized using LETs from $58\text{MeV}\cdot\text{cm}^2/\text{mg}$ to $83\text{MeV}\cdot\text{cm}^2/\text{mg}$. The SEL events were non-destructive and have a very low limiting cross-section of $<3\text{E-}06\text{cm}^2/\text{device}$. The SEL events were considered non-destructive by verifying gross functionality at the beam facility and then by running a full parametric characterization approximately 3-days later.

Using CREME96 we can calculate SEL event rate for a “worst-case” geosynchronous orbit to determine if these units are suitable for space flight applications. Based on the SEL characterization data shown in this report and CREME96, the RAD1419 14-Bit ADC has a “worst-case” geosynchronous SEL rate of $<8\text{E-}08$ events/device-day or an MTBF of 12.5-million days. An equivalent failure in time (FIT) rate is approximately 3 failures/billion device-hours. See Appendix D for the output of the CREME96 run for



the details of the orbit parameters used in the above calculations. Note that the overall reliability of space flight electronics due to failure from random defects in the material is on the order of 10 to 100 FITs. Therefore the probability of an SEL event is much lower than the probability of a random failure of the components in the system. Also note that the code was run for a geosynchronous orbit. Running the code at lower orbit altitudes will cause the FIT rate to drop substantially.

Table 5.1 shows a summary of the single event latch-up data acquired. The table shows the run number, the serial number of the part irradiated, the ion species, the effective LET of the irradiating particle, the case temperature during testing, the number of SEL events observed during the run, the effective fluence and the SEL cross-section. Figure 5.1 shows a plot of the SEL characterization data (solid diamonds) and a Weibull fit to the data. As seen in this figure the units-under-test exhibit a relatively high LET threshold and a very low SEL cross-section per device at the highest LET test of $80\text{MeV}\cdot\text{cm}^2/\text{mg}$.

Figures 5.2 through 5.15 show the supply current data during the SEL runs. In these figures the supply current is plotted as a function of time and the total fluence for each run can be found in Table 5.1. As seen in these figure, when an SEL event occurs the supply current for each supply jumps to approximately 300mA for each supply (+5V nominal supply and the -5V nominal supply). This current is “self regulating”, that is there was no current limiting resistor inline with the power supply pins and the power supply was set to a compliance of 1A. In all cases, the supply current and gross functionality of the device were restored following a power cycle to the unit-under-test.



**SEL Characterization Report
10-xxx 100429 R1.0**

Radiation Assured Devices
5017 N. 30th Street
Colorado Springs, CO 80919
(719) 531-0800

Table 5.1. Summary of the SEL test runs for the RAD1419 14-Bit, 800ksps Sampling A/D Converter with Shutdown. Note that no SEL events are detected with an LET of 55MeV-cm²/mg or less.

RUN Number	Serial Number	Part Type	Temp (°C)	Ion Species/ Energy	Eff. Fluence (ion/cm2)	Effective LET (MeV-cm2/mg)	SEL Events	Effective LET (MeV-cm2/mg)	Cross-Section (cm ²)
6	1	RAD1419	85	Xe 10MeV/n	6.31E+05	83.0	1	83.0	1.58E-06
7	2	RAD1419	85	Xe 10MeV/n	1.17E+06	83.0	1	83.0	8.55E-07
8	3	RAD1419	85	Xe 10MeV/n	3.54E+05	83.0	1	83.0	2.82E-06
9	4	RAD1419	85	Xe 10MeV/n	3.85E+05	83.0	1	83.0	2.60E-06
10	1	RAD1419	85	Xe 10MeV/n	1.29E+06	58.8	1	58.8	7.75E-07
11	2	RAD1419	85	Xe 10MeV/n	5.92E+05	58.8	1	58.8	1.69E-06
12	3	RAD1419	85	Xe 10MeV/n	3.54E+06	58.8	1	58.8	2.82E-07
13	4	RAD1419	85	Xe 10MeV/n	7.19E+05	58.8	1	58.8	1.39E-06
14	1	RAD1419	85	Kr 10MeV/n	1.00E+07	43.6	0	43.6	0.00E+00
15	2	RAD1419	85	Kr 10MeV/n	1.00E+07	43.6	0	43.6	0.00E+00
16	1	RAD1419	85	Kr 10MeV/n	1.00E+07	50.1	0	50.1	0.00E+00
17	2	RAD1419	85	Kr 10MeV/n	1.00E+07	50.1	0	50.1	0.00E+00
18	1	RAD1419	85	Kr 10MeV/n	1.00E+07	55.2	0	55.2	0.00E+00
19	2	RAD1419	85	Kr 10MeV/n	1.01E+06	58.8	1	58.8	9.90E-07
20	3	RAD1419	85	Kr 10MeV/n	1.01E+06	58.8	1	58.8	9.90E-07
21	3	RAD1419	85	Kr 10MeV/n	6.37E+05	67.9	1	67.9	1.57E-06
22	4	RAD1419	86	Kr 10MeV/n	5.10E+05	67.9	1	67.9	1.96E-06
23	2	RAD1419	86	Kr 10MeV/n	4.34E+05	83.1	1	83.1	2.30E-06

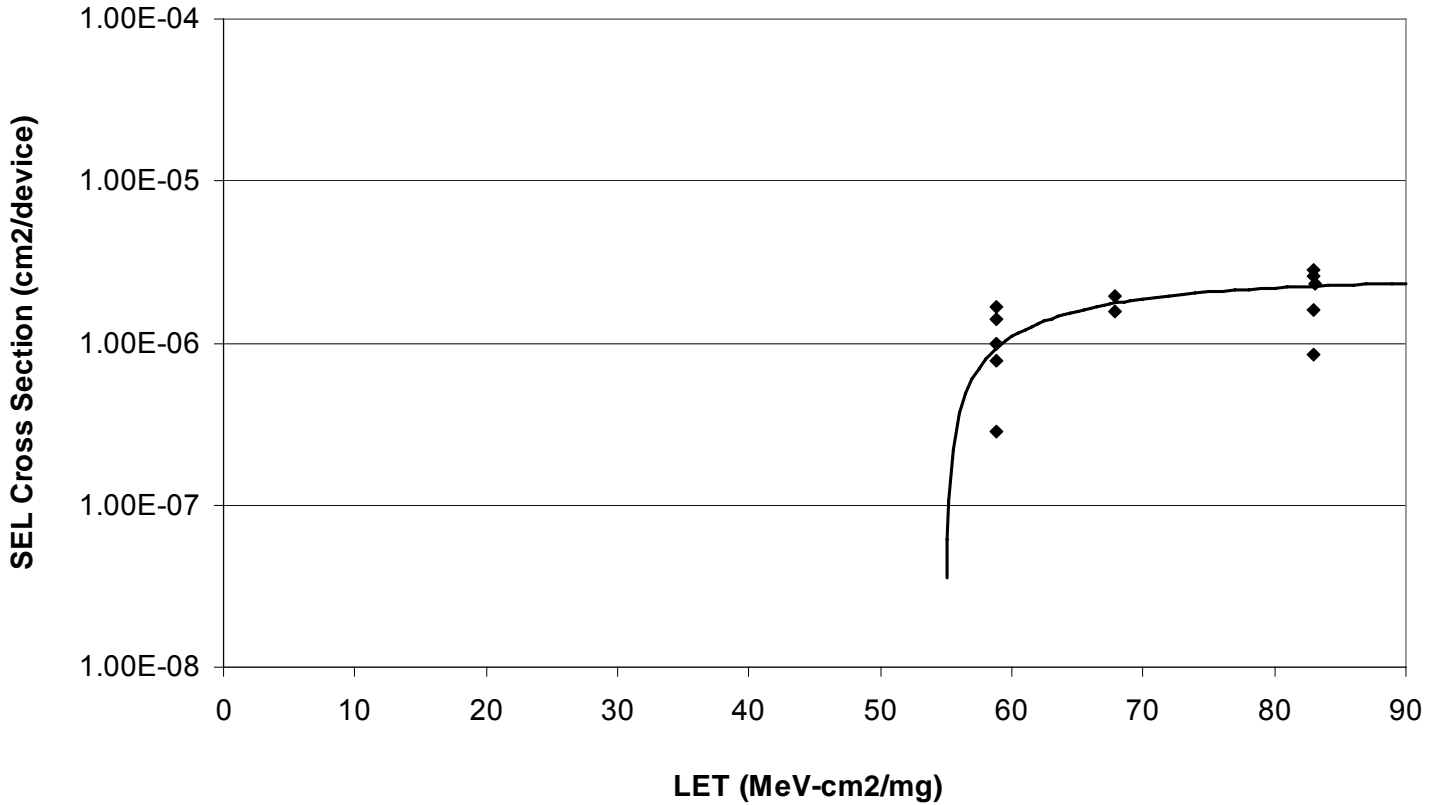


Figure 5.1. SEL cross-section (cm²/device) versus LET for the RAD1419 ADC tested at 85°C and at the worst-case supply potential of ±5.5V. As seen in this figure the units are susceptible to SEL events with a relatively high onset LET of greater than 55MeV-cm²/mg and a very low SEL cross-section per device of approximately 3E-6cm²/device at the maximum tested LET of approximately 80MeV-cm²/mg. Note that this is not the limiting or saturated cross-section since the cross-section may not have fully saturated with increasing LET.

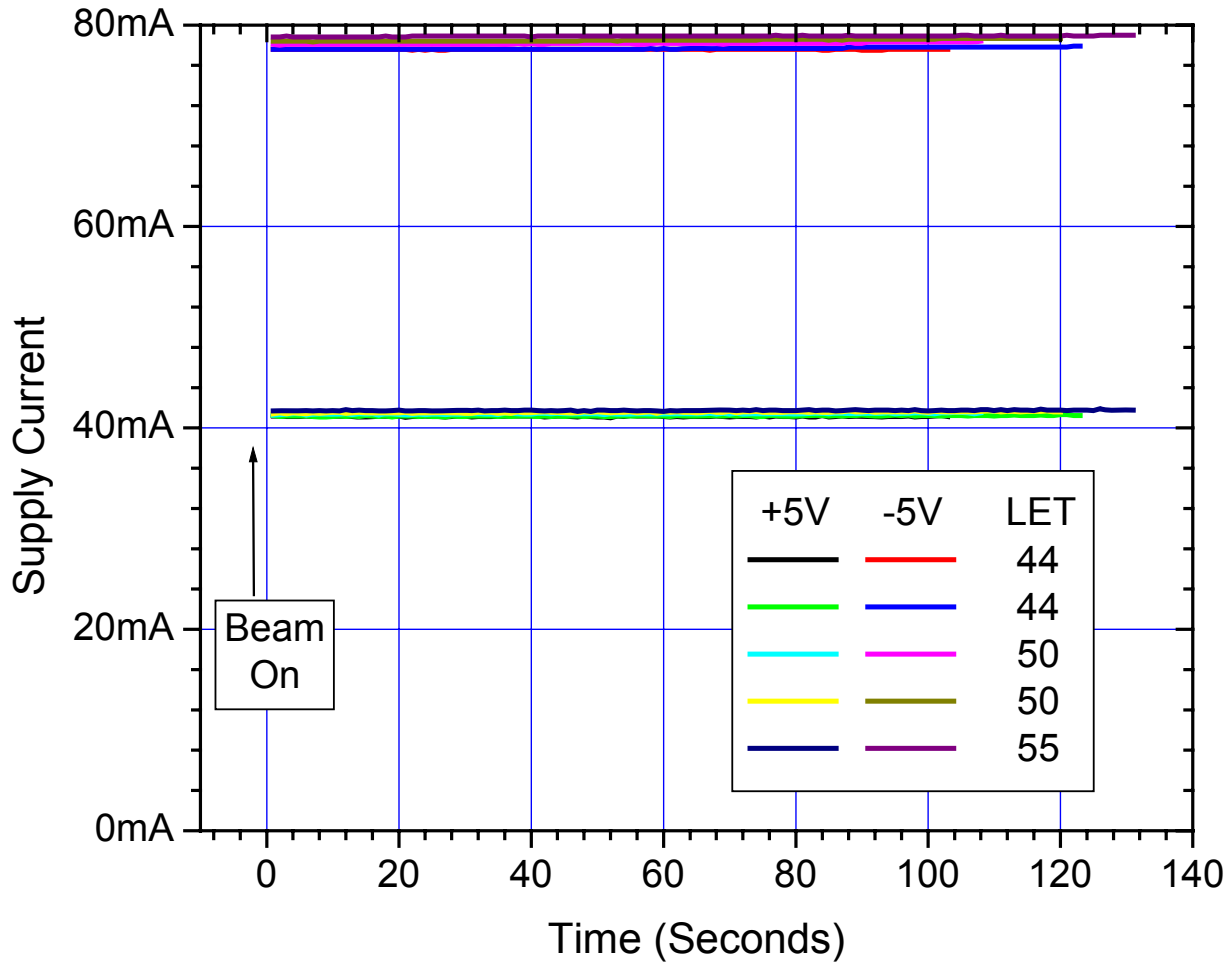


Figure 5.2. Supply current versus time for the RAD1419 14-Bit ADC serial numbers 1 and 2. The units were tested with $\pm 5.5V$ on the V_{S+} and V_{S-} lines and at a case temperature of $85^{\circ}C$. The total fluence to the device can be found in Table 5.1 and was $1E7\text{ions/cm}^2$ for all the runs shown in this figure since no SEL was observed. The data in this figure shows that the units-under-test are SEL “immune” at an effective LET of $55\text{MeV-cm}^2/\text{mg}$ and lower when tested to a total fluence of $1E7\text{ions/cm}^2$. As noted in the text of this report the units remained functional following each run without cycling power and a verification of full parametric performance was performed approximately 3-days following the SEL testing, with all parts passing.

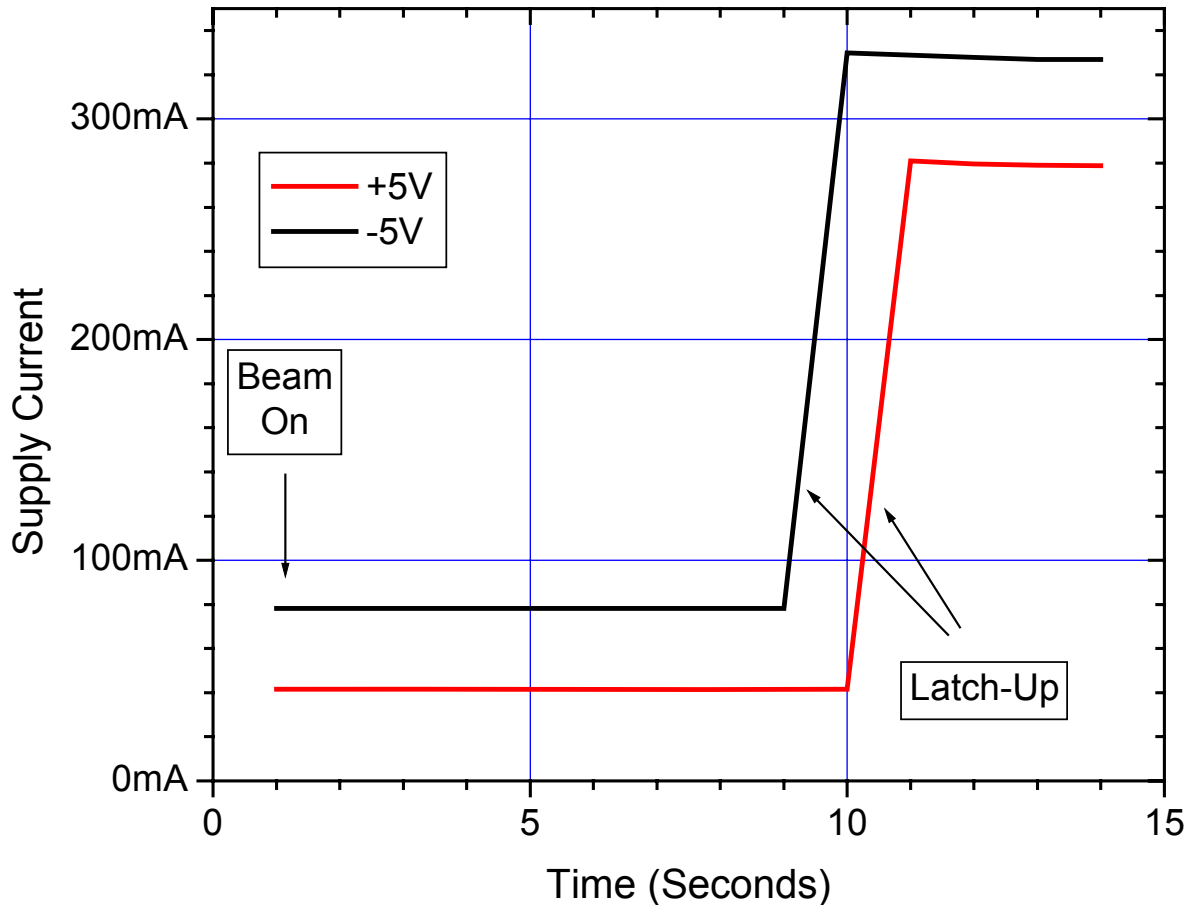


Figure 5.3. Supply current versus time for the RAD1419 14-Bit ADC serial number 1. The unit was tested with $\pm 5.5V$ on the V_{S+} and V_{S-} lines and at a case temperature of $85^{\circ}C$. The total fluence to the device at the onset of SEL can be found in Table 5.1. The data in this figure shows that the units-under-test are susceptible to SEL at an effective LET of approximately $59MeV\text{-}cm^2/mg$. The current is “self limiting to approximately 300mA and, as noted in the text of this report the units remained functional following each run after cycling power. Further a verification of full parametric performance was performed approximately 3-days following the SEL testing, with all parts passing.

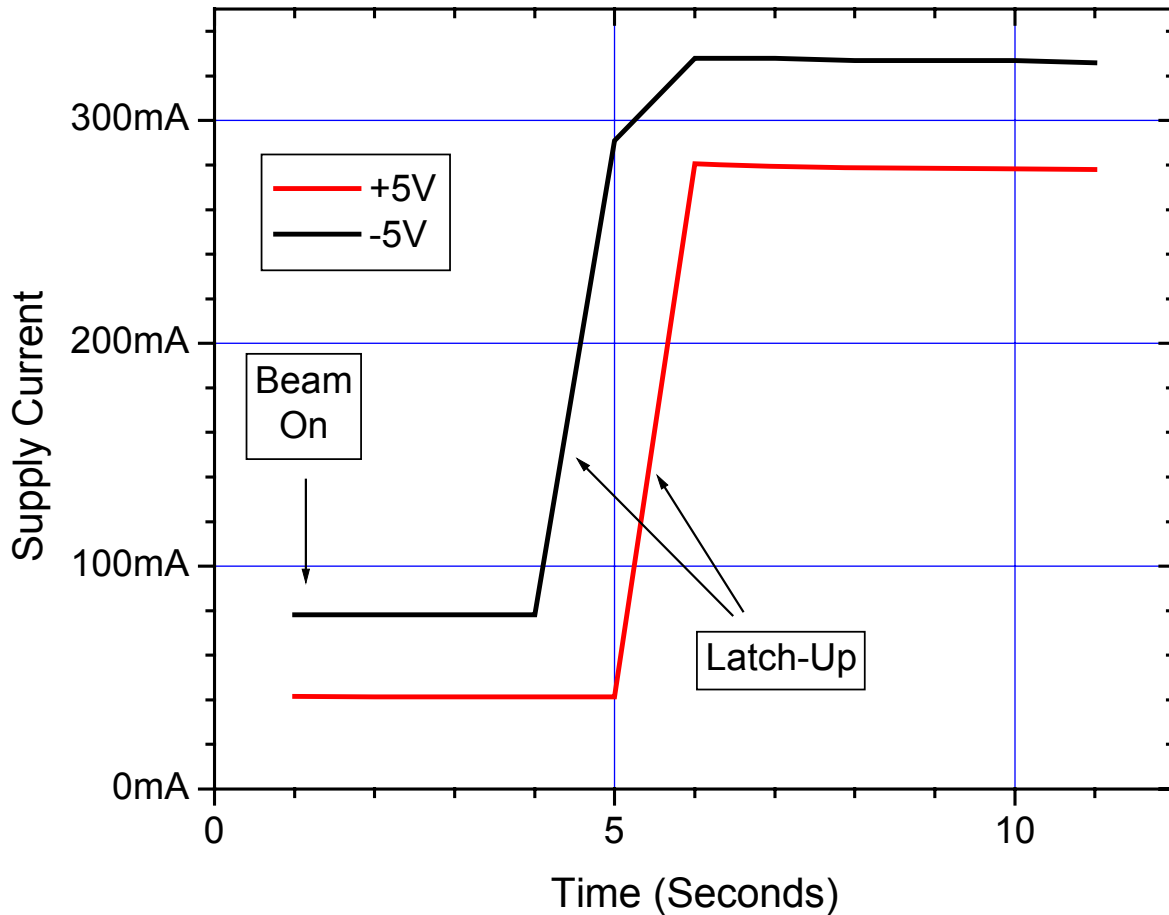


Figure 5.4. Supply current versus time for the RAD1419 14-Bit ADC serial number 2. The unit was tested with $\pm 5.5V$ on the V_{S+} and V_{S-} lines and at a case temperature of $85^{\circ}C$. The total fluence to the device at the onset of SEL can be found in Table 5.1. The data in this figure shows that the units-under-test are susceptible to SEL at an effective LET of approximately $59MeV-cm^2/mg$. The current is “self limiting to approximately 300mA and, as noted in the text of this report the units remained functional following each run after cycling power. Further a verification of full parametric performance was performed approximately 3-days following the SEL testing, with all parts passing.

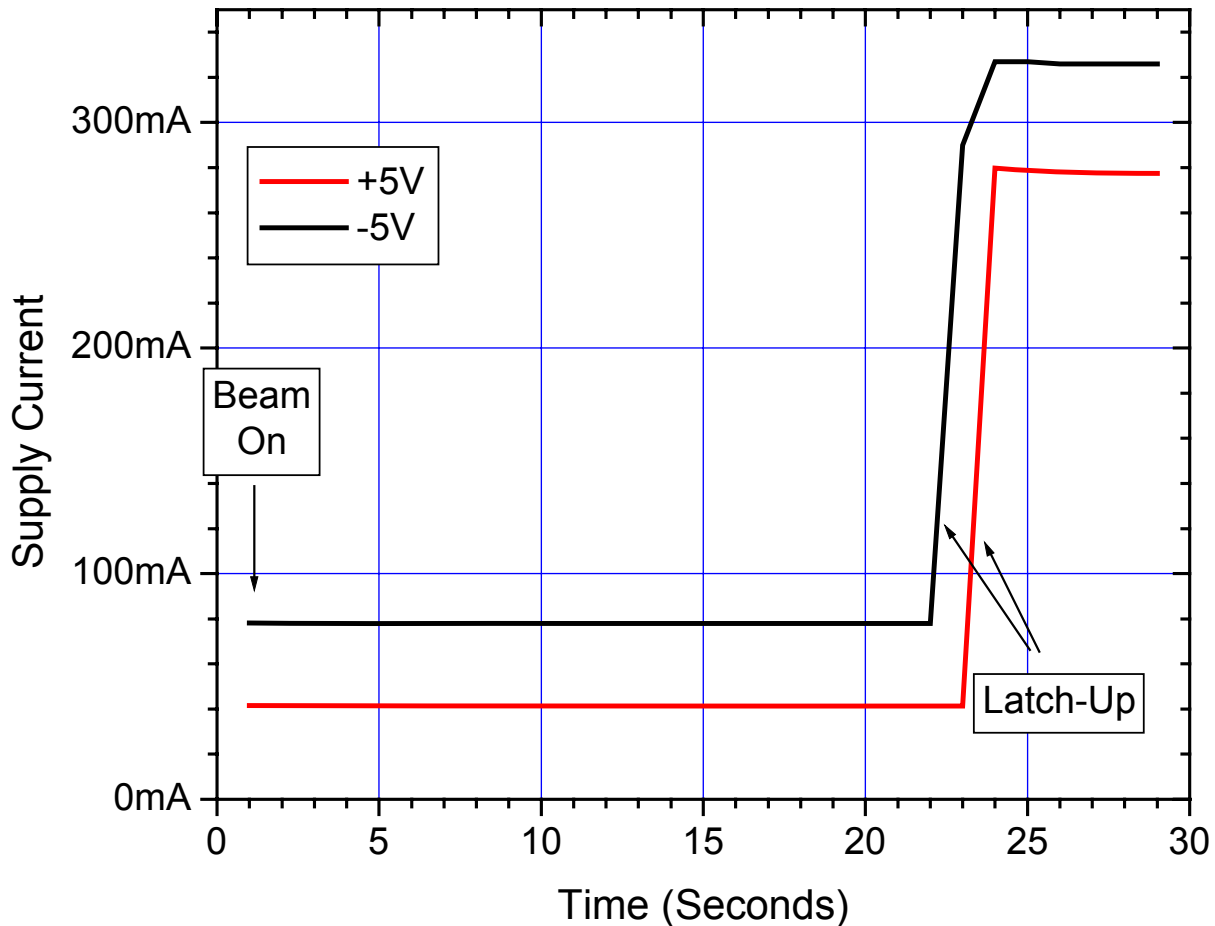


Figure 5.5. Supply current versus time for the RAD1419 14-Bit ADC serial number 3. The unit was tested with $\pm 5.5V$ on the V_{S+} and V_{S-} lines and at a case temperature of $85^{\circ}C$. The total fluence to the device at the onset of SEL can be found in Table 5.1. The data in this figure shows that the units-under-test are susceptible to SEL at an effective LET of approximately $59MeV\text{-}cm^2/mg$. The current is “self limiting to approximately 300mA and, as noted in the text of this report the units remained functional following each run after cycling power. Further a verification of full parametric performance was performed approximately 3-days following the SEL testing, with all parts passing.

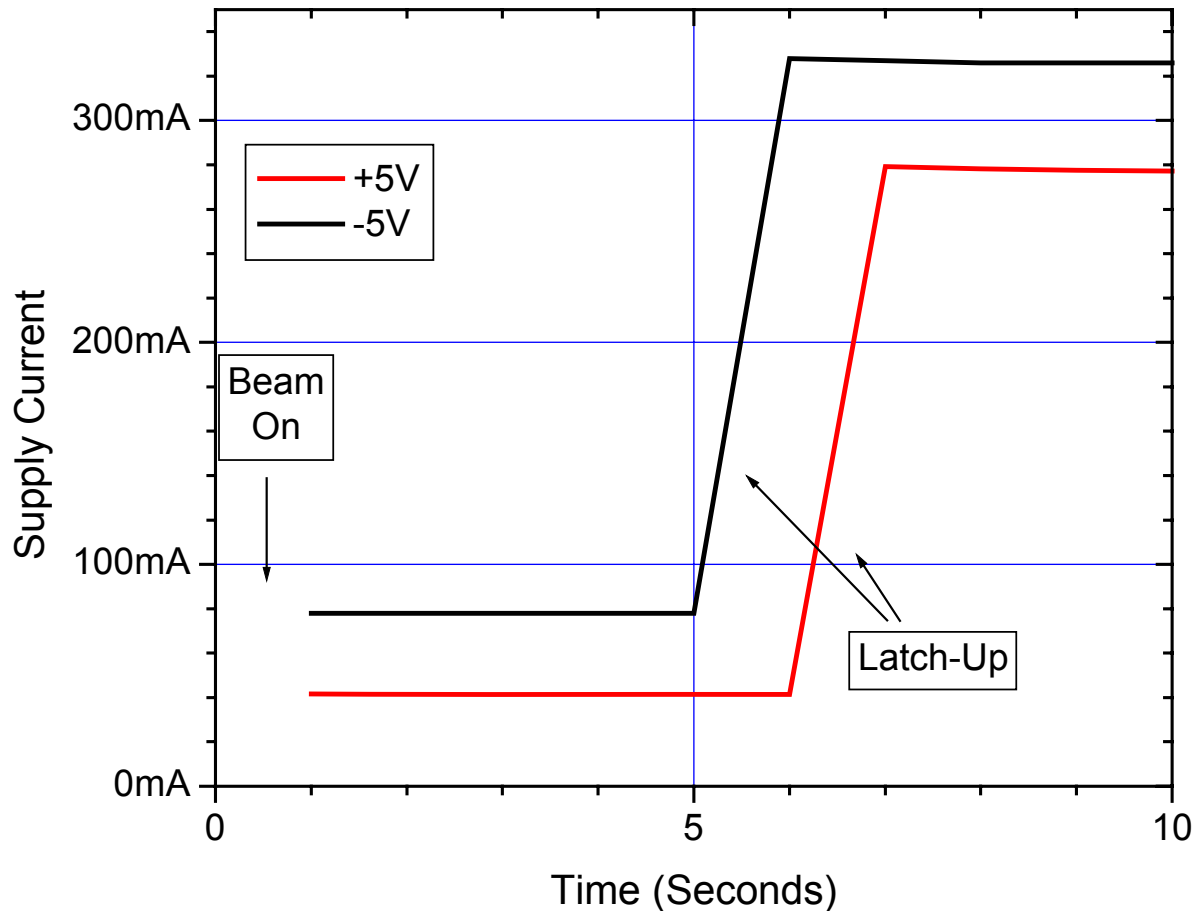


Figure 5.6. Supply current versus time for the RAD1419 14-Bit ADC serial number 4. The unit was tested with $\pm 5.5\text{V}$ on the V_{S+} and V_{S-} lines and at a case temperature of 85°C . The total fluence to the device at the onset of SEL can be found in Table 5.1. The data in this figure shows that the units-under-test are susceptible to SEL at an effective LET of approximately $59\text{MeV}\cdot\text{cm}^2/\text{mg}$. The current is “self limiting to approximately 300mA and, as noted in the text of this report the units remained functional following each run after cycling power. Further a verification of full parametric performance was performed approximately 3-days following the SEL testing, with all parts passing.

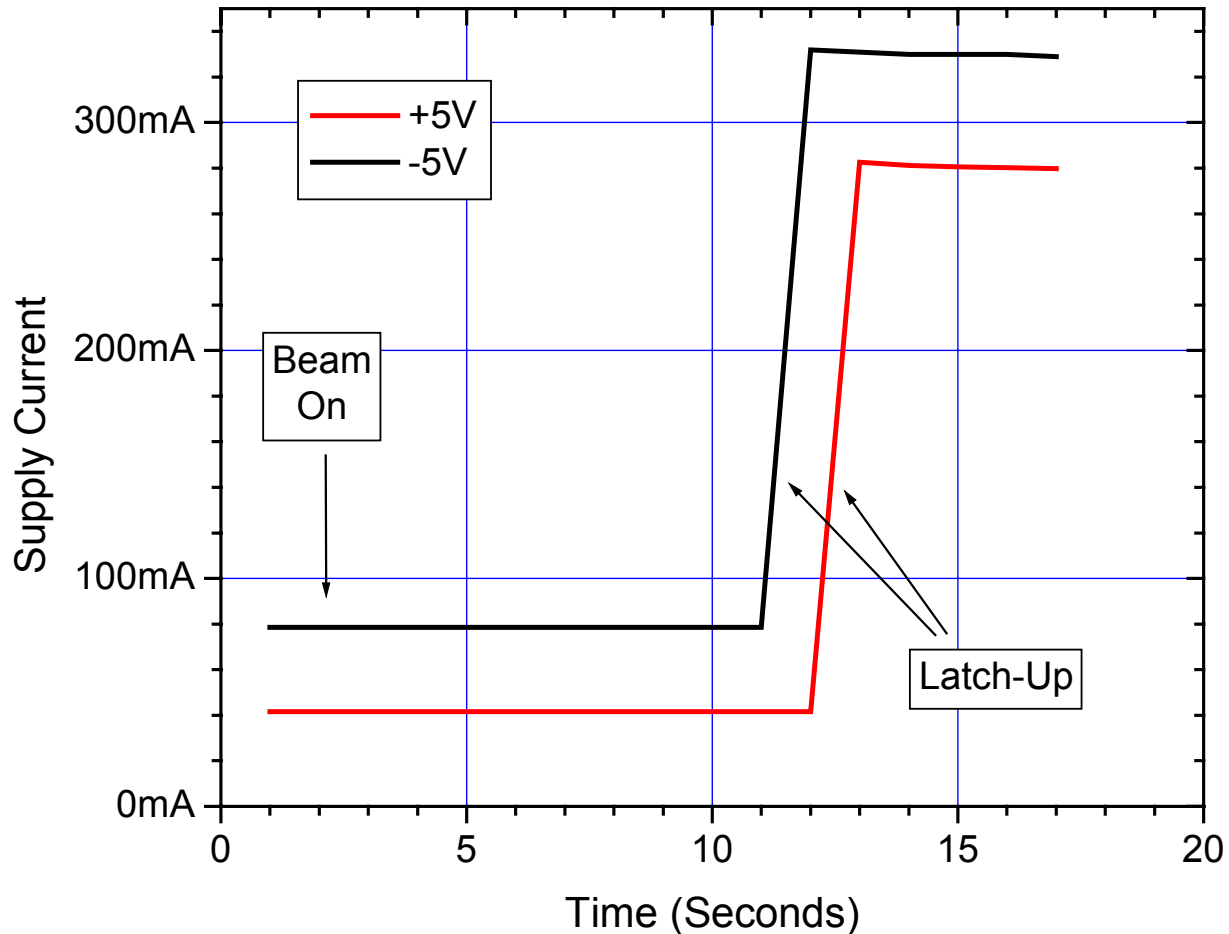


Figure 5.7. Supply current versus time for the RAD1419 14-Bit ADC serial number 2. The unit was tested with $\pm 5.5V$ on the V_{S+} and V_{S-} lines and at a case temperature of $85^{\circ}C$. The total fluence to the device at the onset of SEL can be found in Table 5.1. The data in this figure shows that the units-under-test are susceptible to SEL at an effective LET of approximately $59MeV\text{-}cm^2/mg$. The current is “self limiting to approximately 300mA and, as noted in the text of this report the units remained functional following each run after cycling power. Further a verification of full parametric performance was performed approximately 3-days following the SEL testing, with all parts passing.

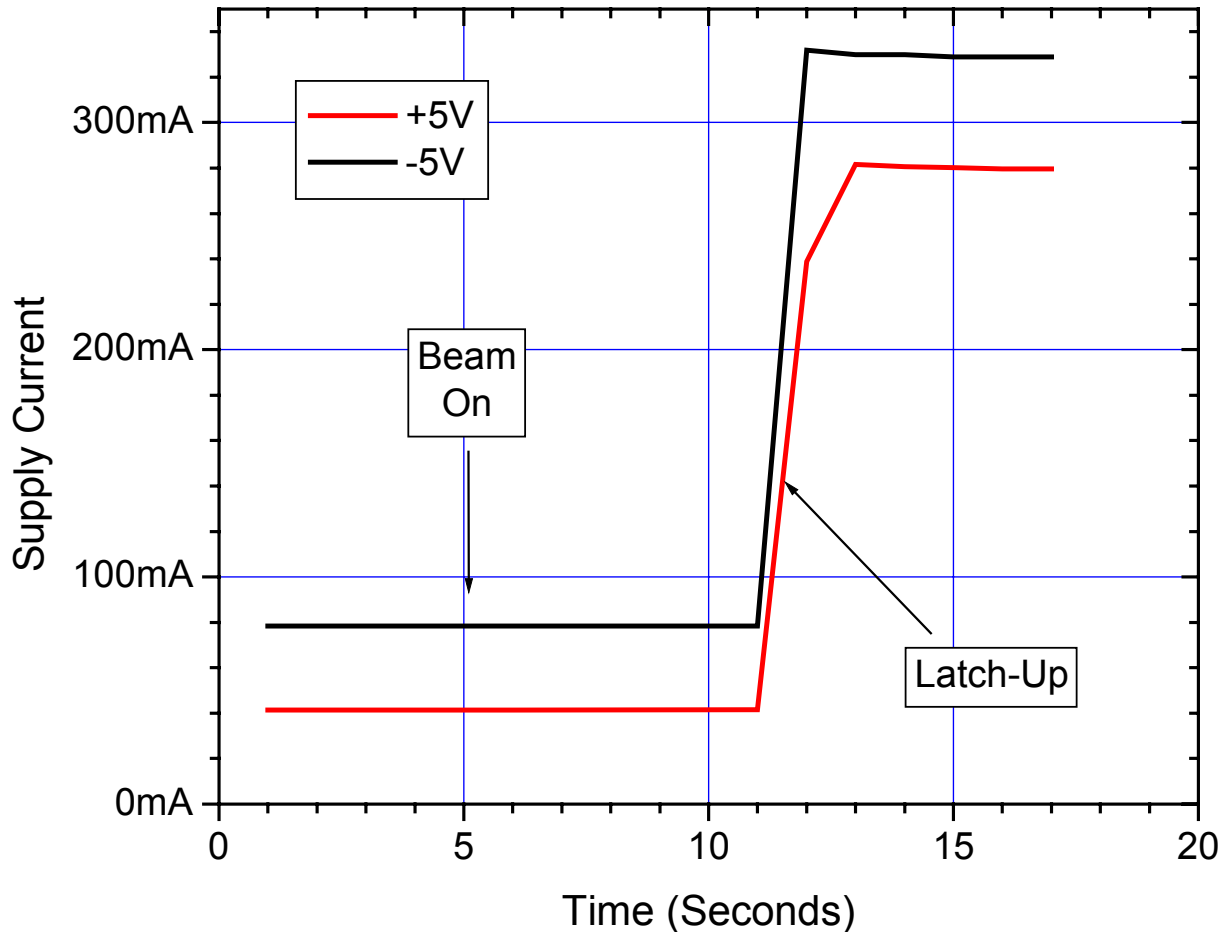


Figure 5.8. Supply current versus time for the RAD1419 14-Bit ADC serial number 3. The unit was tested with $\pm 5.5\text{V}$ on the V_{S+} and V_{S-} lines and at a case temperature of 85°C . The total fluence to the device at the onset of SEL can be found in Table 5.1. The data in this figure shows that the units-under-test are susceptible to SEL at an effective LET of approximately $59\text{MeV}\cdot\text{cm}^2/\text{mg}$. The current is “self limiting to approximately 300mA and, as noted in the text of this report the units remained functional following each run after cycling power. Further a verification of full parametric performance was performed approximately 3-days following the SEL testing, with all parts passing.

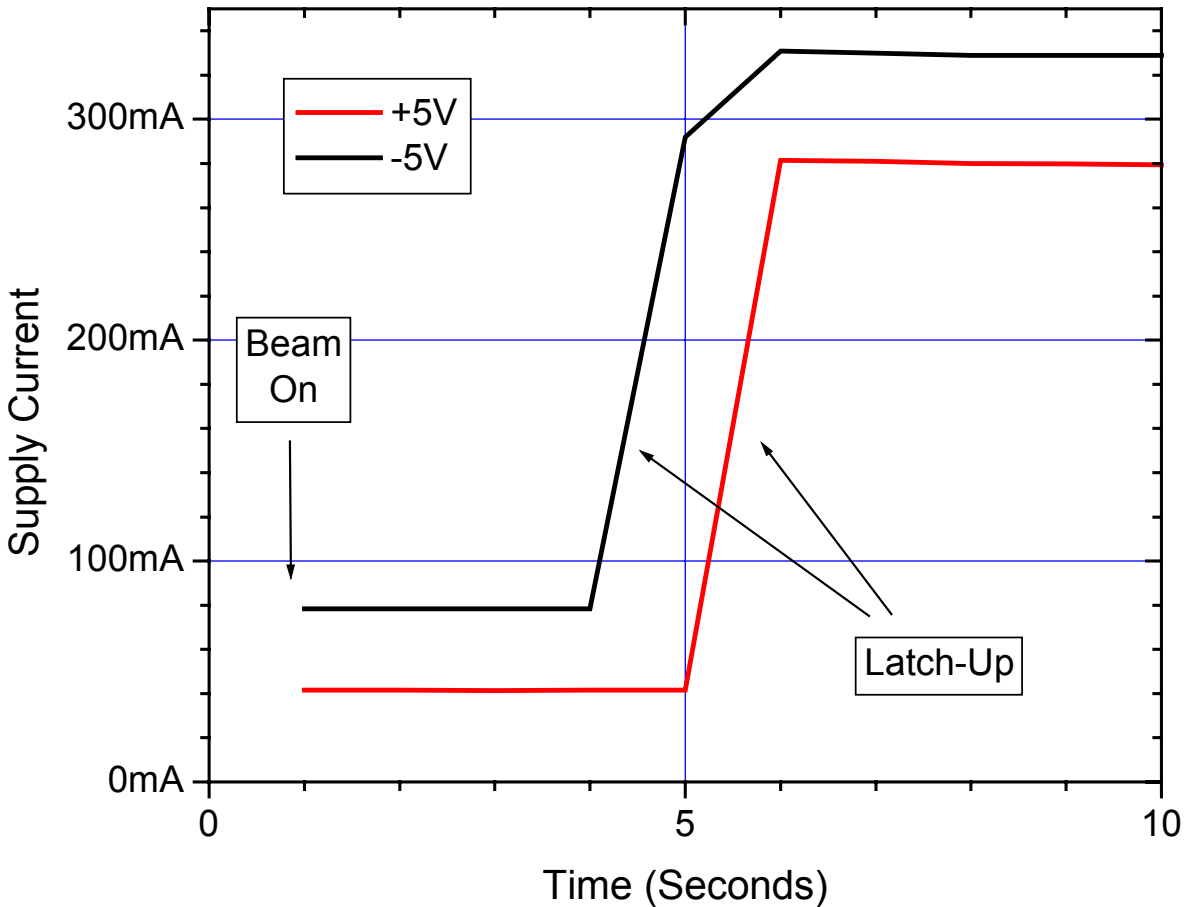


Figure 5.9. Supply current versus time for the RAD1419 14-Bit ADC serial number 3. The unit was tested with $\pm 5.5V$ on the V_{S+} and V_{S-} lines and at a case temperature of $85^{\circ}C$. The total fluence to the device at the onset of SEL can be found in Table 5.1. The data in this figure shows that the units-under-test are susceptible to SEL at an effective LET of approximately $68MeV-cm^2/mg$. The current is “self limiting to approximately 300mA and, as noted in the text of this report the units remained functional following each run after cycling power. Further a verification of full parametric performance was performed approximately 3-days following the SEL testing, with all parts passing.

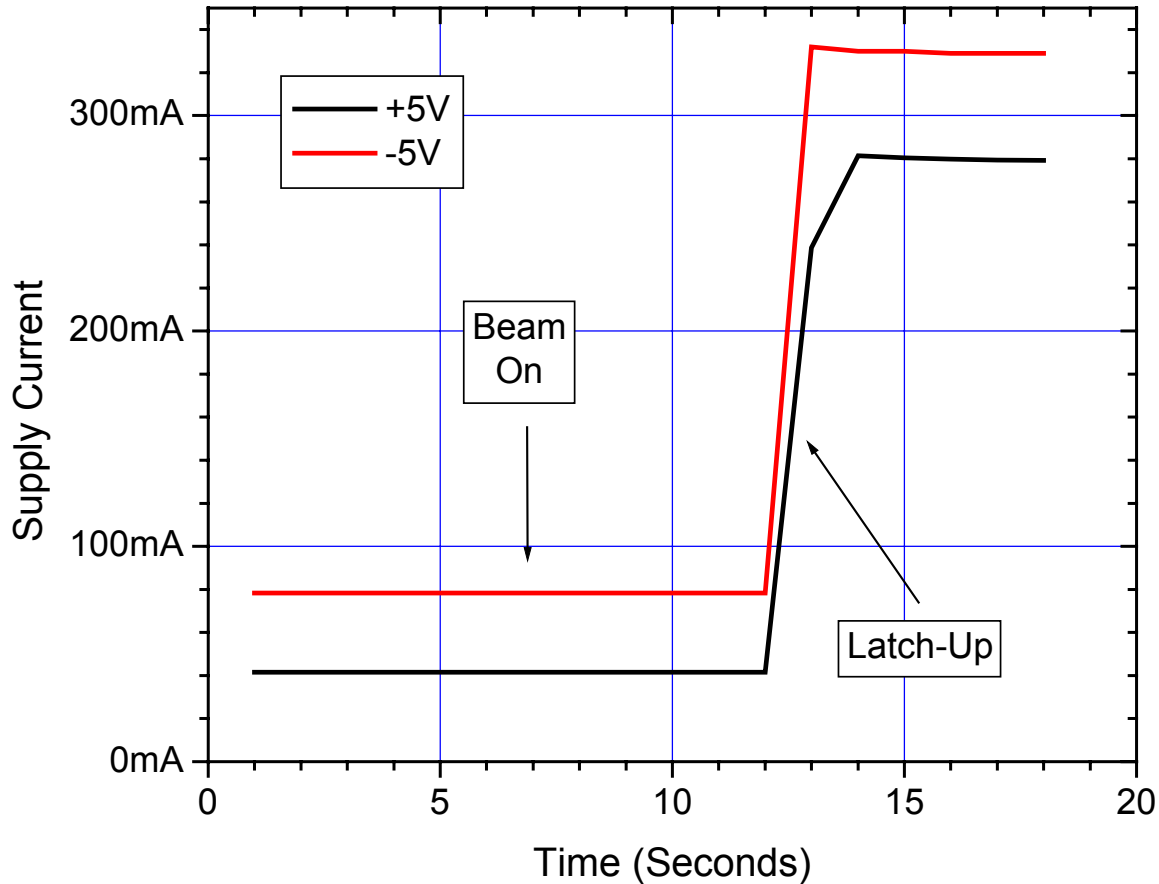


Figure 5.10. Supply current versus time for the RAD1419 14-Bit ADC serial number 4. The unit was tested with $\pm 5.5V$ on the V_{S+} and V_{S-} lines and at a case temperature of $85^{\circ}C$. The total fluence to the device at the onset of SEL can be found in Table 5.1. The data in this figure shows that the units-under-test are susceptible to SEL at an effective LET of approximately $68MeV\text{-}cm^2/mg$. The current is “self limiting to approximately 300mA and, as noted in the text of this report the units remained functional following each run after cycling power. Further a verification of full parametric performance was performed approximately 3-days following the SEL testing, with all parts passing.

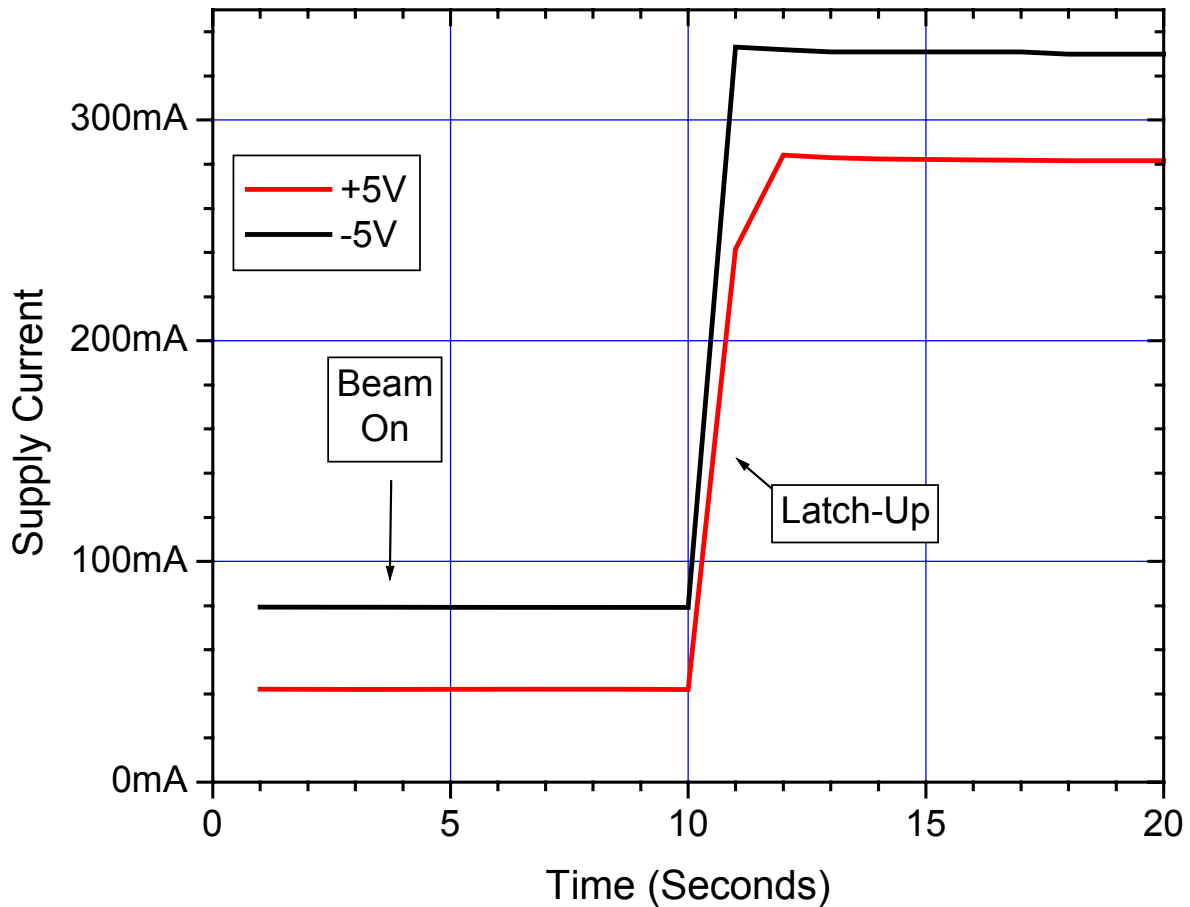


Figure 5.11. Supply current versus time for the RAD1419 14-Bit ADC serial number 1. The unit was tested with $\pm 5.5\text{V}$ on the V_{S+} and V_{S-} lines and at a case temperature of 85°C . The total fluence to the device at the onset of SEL can be found in Table 5.1. The data in this figure shows that the units-under-test are susceptible to SEL at an effective LET of approximately $83\text{MeV}\cdot\text{cm}^2/\text{mg}$. The current is “self limiting to approximately 300mA and, as noted in the text of this report the units remained functional following each run after cycling power. Further a verification of full parametric performance was performed approximately 3-days following the SEL testing, with all parts passing.

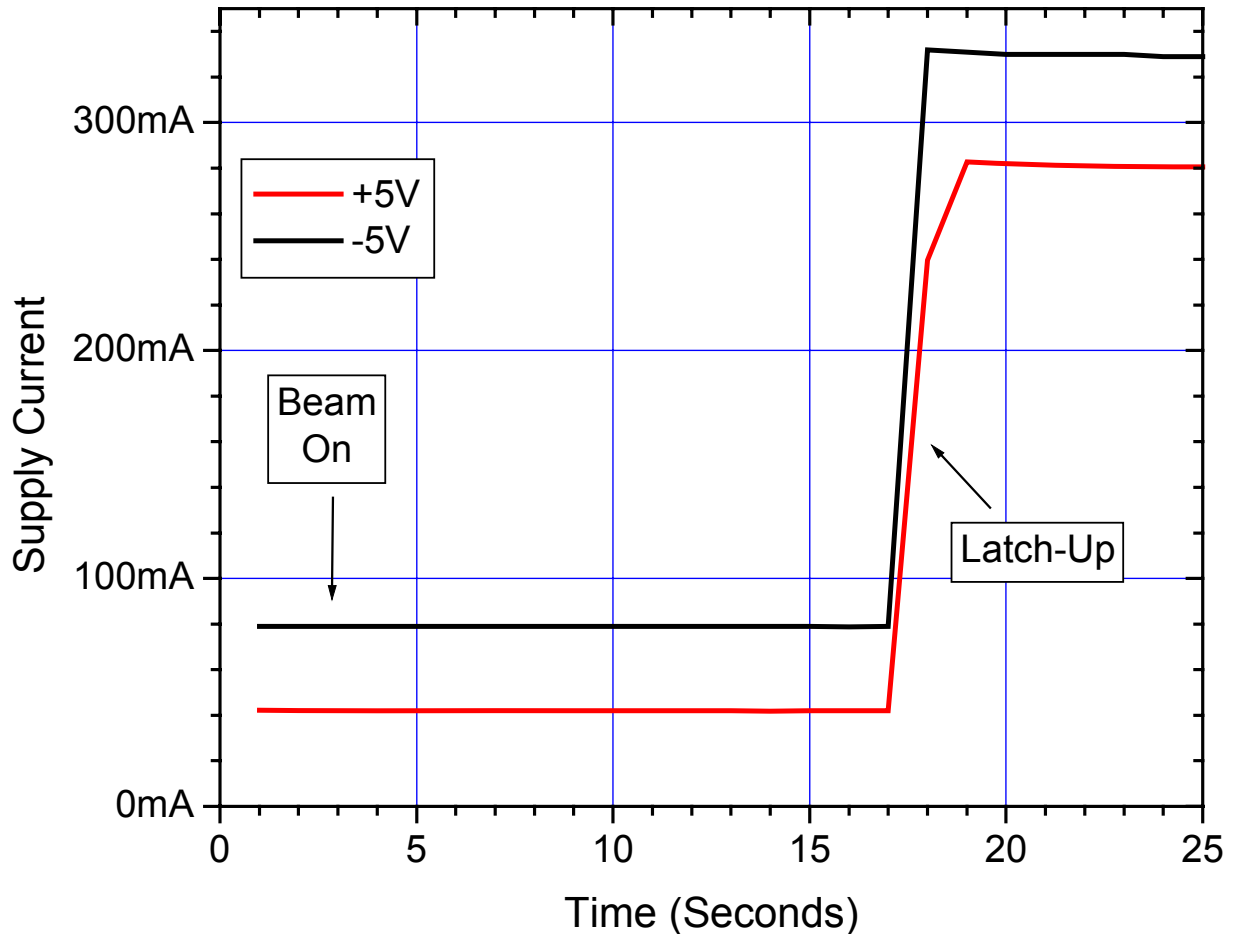


Figure 5.12. Supply current versus time for the RAD1419 14-Bit ADC serial number 2. The unit was tested with $\pm 5.5V$ on the V_{S+} and V_{S-} lines and at a case temperature of $85^{\circ}C$. The total fluence to the device at the onset of SEL can be found in Table 5.1. The data in this figure shows that the units-under-test are susceptible to SEL at an effective LET of approximately $83MeV\text{-}cm^2/mg$. The current is “self limiting to approximately 300mA and, as noted in the text of this report the units remained functional following each run after cycling power. Further a verification of full parametric performance was performed approximately 3-days following the SEL testing, with all parts passing.

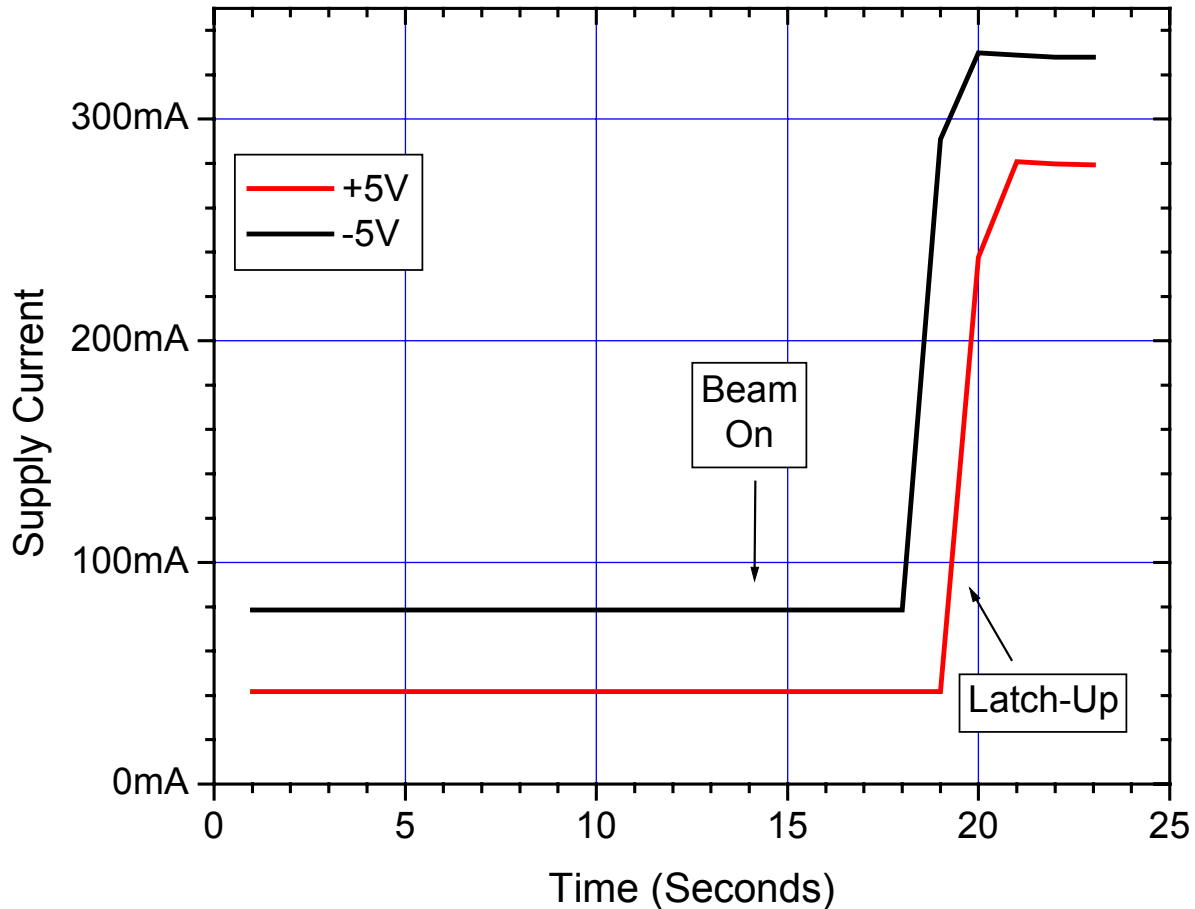


Figure 5.13. Supply current versus time for the RAD1419 14-Bit ADC serial number 3. The unit was tested with $\pm 5.5\text{V}$ on the V_{S+} and V_{S-} lines and at a case temperature of 85°C . The total fluence to the device at the onset of SEL can be found in Table 5.1. The data in this figure shows that the units-under-test are susceptible to SEL at an effective LET of approximately $83\text{MeV}\cdot\text{cm}^2/\text{mg}$. The current is “self limiting to approximately 300mA and, as noted in the text of this report the units remained functional following each run after cycling power. Further a verification of full parametric performance was performed approximately 3-days following the SEL testing, with all parts passing.

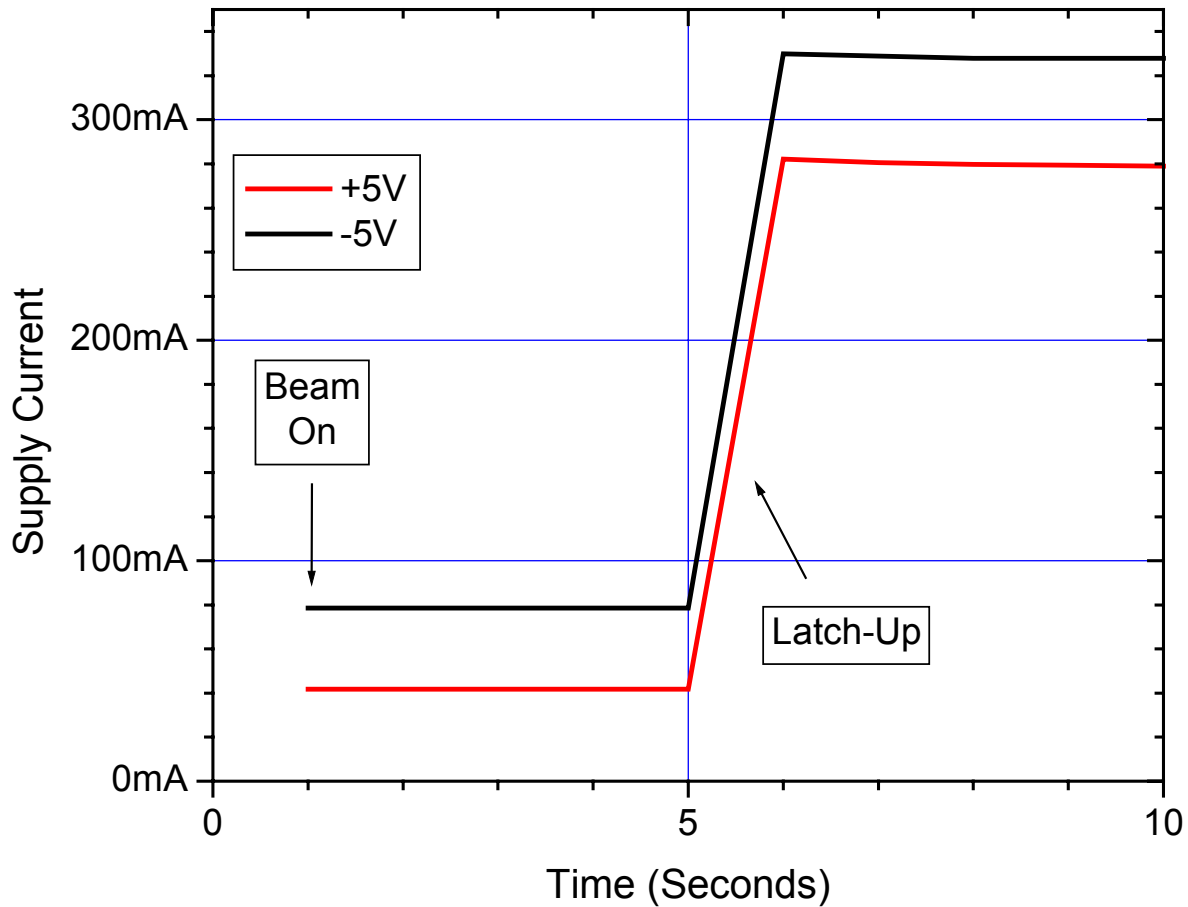


Figure 5.14. Supply current versus time for the RAD1419 14-Bit ADC serial number 4. The unit was tested with $\pm 5.5V$ on the V_{S+} and V_{S-} lines and at a case temperature of $85^{\circ}C$. The total fluence to the device at the onset of SEL can be found in Table 5.1. The data in this figure shows that the units-under-test are susceptible to SEL at an effective LET of approximately $83MeV\text{-}cm^2/mg$. The current is “self limiting to approximately 300mA and, as noted in the text of this report the units remained functional following each run after cycling power. Further a verification of full parametric performance was performed approximately 3-days following the SEL testing, with all parts passing.

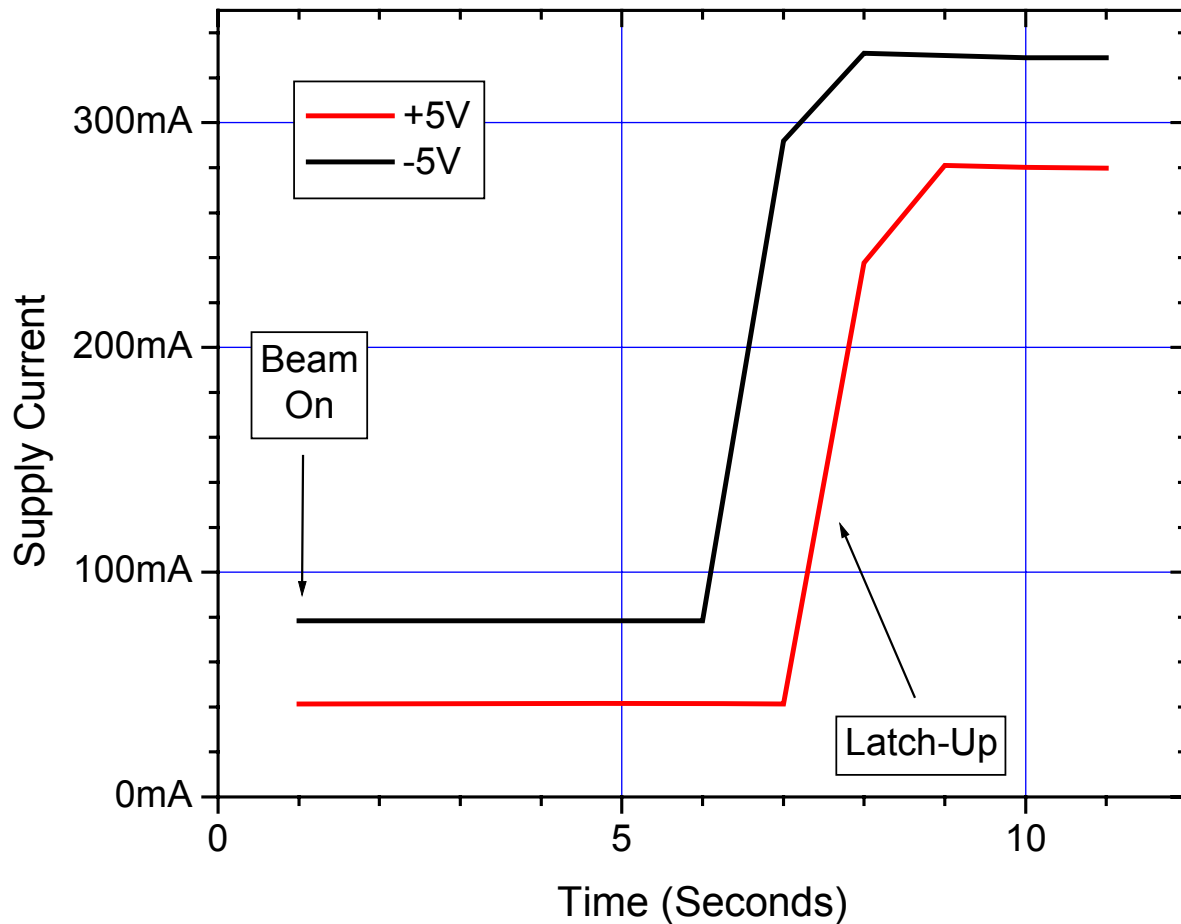


Figure 5.15. Supply current versus time for the RAD1419 14-Bit ADC serial number 2. The unit was tested with $\pm 5.5V$ on the V_{S+} and V_{S-} lines and at a case temperature of $85^{\circ}C$. The total fluence to the device at the onset of SEL can be found in Table 5.1. The data in this figure shows that the units-under-test are susceptible to SEL at an effective LET of approximately $83MeV\text{-}cm^2/mg$. The current is “self limiting to approximately 300mA and, as noted in the text of this report the units remained functional following each run after cycling power. Further a verification of full parametric performance was performed approximately 3-days following the SEL testing, with all parts passing.



6.0. Summary/Conclusions

The single event latch-up testing described in this final report was performed at the Lawrence Berkeley National Laboratories (LBNL) using the 88-Inch Cyclotron. The 88-Inch Cyclotron is operated by the University of California for the US Department of Energy (DOE) and is a K=140 sector-focused cyclotron with both light- and heavy-ion capabilities. Protons and other light-ions are available at high intensities (10-20 μ A) up to maximum energies of 55 MeV (protons), 65 MeV (deuterons), 135 MeV (3He) and 140 MeV (4He). Most heavy ions through uranium can be accelerated to maximum energies, which vary with the mass and charge state.

The RAD1419 14-Bit, 800ksps Sampling A/D Converter with Shutdown described in this final report was irradiated using Kr and Xe with a split positive supply potential of 5.5V and at a maximum case temperature of 85°C. The 10MeV/n beam was used to provide sufficient range in silicon while meeting the maximum LET requirements of the program. The devices were irradiated to a minimum fluence of 1E7ion/cm² for each run or until a latch-up event was detected. The flux varied somewhat during the testing, but was consistently targeted to between 2E5ion/cm²-s and 5E5ion/cm²-s.

The RAD1419 14-Bit, 800ksps Sampling A/D Converter SEL test units-under-test did not exhibit latch-up at any LETs of 55MeV-cm²/mg or lower. SEL events were recorded and characterized using LETs from 58MeV-cm²/mg to 83MeV-cm²/mg. The SEL events were non-destructive and have a very low limiting cross-section of <3E-06cm²/device. The SEL events were considered non-destructive by verifying gross functionality at the beam facility and then by running a full parametric characterization approximately 3-days later.

Using CREME96 we can calculate the SEL event rate for a “worst-case” geosynchronous orbit to determine if these units are suitable for space flight applications. Based on the SEL characterization data shown in this report and CREME96, the RAD1419 14-Bit ADC has a “worst-case” geosynchronous SEL rate of <8E-08 events/device-day or an MTBF of 12.5-million days. An equivalent failure in time (FIT) rate is approximately 3 failures/billion device-hours. Note that the overall reliability of space flight electronics due to failure from random defects in the material is on the order of 10 to 100 FITs. Therefore the probability of an SEL event is much lower than the probability of a random failure of the components in the system. Also note that the code was run for a geosynchronous orbit. Running the code at lower orbit altitudes will cause the FIT rate to drop substantially.



Appendix A: Photograph of Sample Unit-Under-Test to Show Device Traceability





Appendix B: SEL Bias Connections

Biased Samples:

FUNCTION	PIN NUMBER	BIAS CONNECTIONS DURING IRRADIATION
+A _{IN}	1	+2.5V, 1000pF Ceramic to -A _{IN}
-A _{IN}	2	GND
V _{REF}	3	10μF Ceramic to GND
REFCOMP	4	10μF Ceramic to GND
AGND	5	GND
D13 (MSB)	6	Open
D12	7	Open
D11	8	Open
D10	9	Open
D9	10	Open
D8	11	Open
D7	12	Open
D6	13	Open
DGND	14	GND
D5	15	Open
D4	16	Open
D3	17	Open
D2	18	Open
D1	19	Open
D0	20	Open
SHDN/	21	+5.5 V ± 0.15 V
RD/	22	GND
CONVST/	23	500 kHz Square Wave @ 5 % Duty Cycle
CS/	24	GND
BUSY/	25	Open
V _{SS}	26	-5.5 V ± 0.15 V, 10μF Ceramic to GND
DV _{DD}	27	Pin 28
AV _{DD}	28	+5.5 V ± 0.15 V, 10μF Ceramic to GND



28-Pin Flat Pack (F)

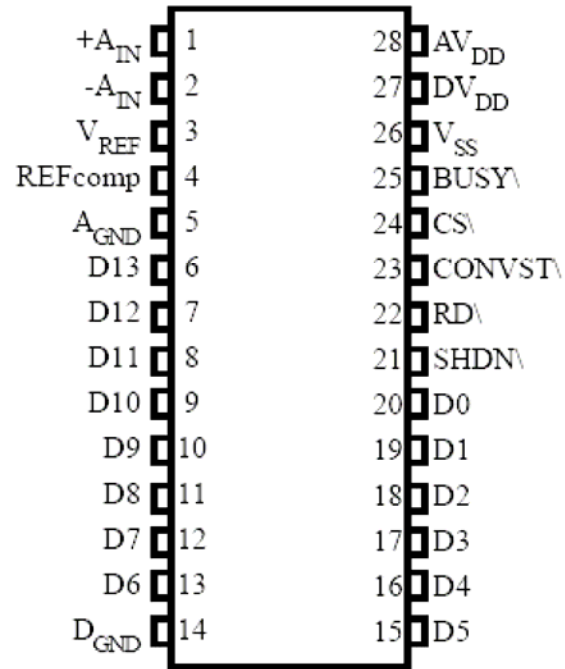


Figure B.1. RAD1419 28-Pin Flat pack package drawing (for reference only).



Appendix C: Post-SEL Electrical Test Parameters and Conditions

All electrical tests for this device are performed on one of Radiation Assured Device's LTS2020 Test Systems. The LTS2020 Test System is a programmable parametric tester that provides parameter measurements for a variety of digital, analog and mixed signal products including voltage regulators, voltage comparators, D to A and A to D converters. The LTS2020 Test System achieves accuracy and sensitivity through the use of software self-calibration and an internal relay matrix with separate family boards and custom personality adapter boards. The tester uses this relay matrix to connect the required test circuits, select the appropriate voltage / current sources and establish the needed measurement loops for all the tests performed. The measured parameters and test conditions are shown in Table C.1.

A listing of the measurement precision/resolution for each parameter is shown in Table C.2. The precision/resolution values were obtained either from test data or from the DAC resolution of the LTS-2020. To generate the precision/resolution shown in Table C.2, one of the units-under-test was tested repetitively (a total of 10-times with re-insertion between tests) to obtain the average test value and standard deviation. Using this test data MIL-HDBK-814 90/90 KTL statistics were applied to the measured standard deviation to generate the final measurement range. This value encompasses the precision/resolution of all aspects of the test system, including the LTS2020 mainframe, family board, socket assembly and DUT board as well as insertion error. In some cases, the measurement resolution is limited by the internal DACs, which results in a measured standard deviation of zero. In these instances the precision/resolution will be reported back as the LSB of the DAC.



Table C.1. Measured post-SEL parameters and test conditions for the RAD1419.

Parameter	Test Condition
Power Supply Current	SHDN=V _{CC} , CS=0
Power Supply Current, Nap Mode	SHDN=0 CS=0
Power Supply Current, Sleep Mode	SHDN=0 CS=1
Power Supply Current	SHDN=1 CS=0
Power Supply Current, Nap Mode	SHDN=0 CS=0
Power Supply Current, Sleep Mode	SHDN=0 CS=1
VREF	IOUT = 0
VOL D0-D13	IOUT = 1.6mA
VOH D0-D13	IOUT = -200μA
VOH0p2MA_BUSY	IOUT = -200μA
IOZH D0-D13	VOUT=5V, CS/ = High
IOZLVO D0-13	VOUT=0V, CS/ = High
IIL CS	VIN=0V
IIL RD	VIN=0V
IIL SHDN	VIN=0V
IIL CONVST	VIN=0V
IIH CS	VIN=5V
IIH RD	VIN=5V
IIH SHDN	VIN=5V
IIH CONVST	VIN=5V
+Analog Input Leakage Current	VIN=2.5V
-Analog Input Leakage Current	VIN=-2.5V
Bipolar Offset	VDD = 5V, VSS = - 5V
Bipolar Gain (Full Scale) Error	VDD = 5V, VSS = - 5V
Integral Linearity Error-Positive	VDD = 5V, VSS = - 5V
Integral Linearity Error-Negative	VDD = 5V, VSS = - 5V
Differential Linearity Error-Long	VDD = 5V, VSS = - 5V
Differential Linearity Error-Short	VDD = 5V, VSS = - 5V
SFDR	100kHz Input Signal
THD	100kHz Input Signal, First 5 Harmonics
SINAD	100kHz Input Signal



Table C.2. Measured post-SEL parameters, pre-irradiation specifications and measurement resolution/precision for the RAD1419.

Parameter	Spec Min	Spec Max	Precision (stdev*2.065)
ICCSHDN=1CS=0		2.00E-02	±6.14E-05
ICCSHDN=0CS=0		3.00E-03	±8.71E-06
ICCSHDN=0CS=1		3.00E-03	±1.07E-05
IEESHDN=1CS=0	-3.00E-02		±5.40E-05
IEESHDN=0CS=0	-5.00E-04		±8.26E-06
IEESHDN=0CS=1	-1.00E-04		±1.81E-07
VREF	2.48E+00	2.52E+00	±9.67E-16
VOL1p6MA_D0		4.00E-01	±1.63E-03
VOL1p6MA_D1		4.00E-01	±1.46E-03
VOL1p6MA_D2		4.00E-01	±1.75E-03
VOL1p6MA_D3		4.00E-01	±1.63E-03
VOL1p6MA_D4		4.00E-01	±1.17E-03
VOL1p6MA_D5		4.00E-01	±1.63E-03
VOL1p6MA_D6		4.00E-01	±1.39E-03
VOL1p6MA_D7		4.00E-01	±1.52E-03
VOL1p6MA_D8		4.00E-01	±1.17E-03
VOL1p6MA_D9		4.00E-01	±1.52E-03
VOL1p6MA_D10		4.00E-01	±1.52E-03
VOL1p6MA_D11		4.00E-01	±1.31E-03
VOL1p6MA_D12		4.00E-01	±1.17E-03
VOL1p6MA_D13		4.00E-01	±1.52E-03
VOH0p2MA_D0	4.00E+00		±4.27E-03
VOH0p2MA_D1	4.00E+00		±3.99E-03
VOH0p2MA_D2	4.00E+00		±4.35E-03
VOH0p2MA_D3	4.00E+00		±3.99E-03
VOH0p2MA_D4	4.00E+00		±3.99E-03
VOH0p2MA_D5	4.00E+00		±3.48E-03
VOH0p2MA_D6	4.00E+00		±4.27E-03
VOH0p2MA_D7	4.00E+00		±3.48E-03
VOH0p2MA_D8	4.00E+00		±3.48E-03
VOH0p2MA_D9	4.00E+00		±4.27E-03
VOH0p2MA_D10	4.00E+00		±2.61E-03
VOH0p2MA_D11	4.00E+00		±1.00E-03
VOH0p2MA_D12	4.00E+00		±1.00E-03
VOH0p2MA_BUSY	4.00E+00		±1.00E-03



**SEL Characterization Report
10-xxx 100429 R1.0**

Radiation Assured Devices
5017 N. 30th Street
Colorado Springs, CO 80919
(719) 531-0800

VOH0p2MA_D13	4.00E+00		±3.48E-03
IOZHVO=5V_D0	-1.00E-05	1.00E-05	±2.95E-09
IOZHVO=5V_D1	-1.00E-05	1.00E-05	±5.22E-09
IOZHVO=5V_D2	-1.00E-05	1.00E-05	±3.54E-09
IOZHVO=5V_D3	-1.00E-05	1.00E-05	±3.52E-09
IOZHVO=5V_D4	-1.00E-05	1.00E-05	±3.92E-09
IOZHVO=5V_D5	-1.00E-05	1.00E-05	±4.89E-09
IOZHVO=5V_D6	-1.00E-05	1.00E-05	±4.87E-09
IOZHVO=5V_D7	-1.00E-05	1.00E-05	±5.08E-09
IOZHVO=5V_D8	-1.00E-05	1.00E-05	±6.06E-09
IOZHVO=5V_D9	-1.00E-05	1.00E-05	±5.78E-09
IOZHVO=5V_D10	-1.00E-05	1.00E-05	±3.65E-09
IOZHVO=5V_D11	-1.00E-05	1.00E-05	±5.06E-09
IOZHVO=5V_D12	-1.00E-05	1.00E-05	±4.27E-09
IOZHVO=5V_D13	-1.00E-05	1.00E-05	±4.91E-09
IOZLVO=0V_D0	-1.00E-05	1.00E-05	±3.48E-09
IOZLVO=0V_D1	-1.00E-05	1.00E-05	±4.89E-09
IOZLVO=0V_D2	-1.00E-05	1.00E-05	±3.89E-09
IOZLVO=0V_D3	-1.00E-05	1.00E-05	±3.43E-09
IOZLVO=0V_D4	-1.00E-05	1.00E-05	±4.27E-09
IOZLVO=0V_D5	-1.00E-05	1.00E-05	±3.26E-09
IOZLVO=0V_D6	-1.00E-05	1.00E-05	±3.57E-09
IOZLVO=0V_D7	-1.00E-05	1.00E-05	±2.27E-09
IOZLVO=0V_D8	-1.00E-05	1.00E-05	±2.58E-09
IOZLVO=0V_D9	-1.00E-05	1.00E-05	±3.43E-09
IOZLVO=0V_D10	-1.00E-05	1.00E-05	±3.40E-09
IOZLVO=0V_D11	-1.00E-05	1.00E-05	±2.39E-09
IOZLVO=0V_D12	-1.00E-05	1.00E-05	±2.83E-09
IOZLVO=0V_D13	-1.00E-05	1.00E-05	±3.65E-09
III0V_CS	-1.00E-05	1.00E-05	±3.48E-09
III0V_RD	-1.00E-05	1.00E-05	±2.76E-09
III0V_SHDN	-1.00E-05	1.00E-05	±3.38E-09
III0V_CONVST	-1.00E-05	1.00E-05	±1.63E-09
IIH5V_CS	-1.00E-05	1.00E-05	±1.63E-09
IIH5V_RD	-1.00E-05	1.00E-05	±2.93E-09
IIH5V_SHDN	-1.00E-05	1.00E-05	±1.44E-09
IIH5V_CONVST	-1.00E-05	1.00E-05	±3.62E-09
IINp2p5VAIN	-1.00E-06	1.00E-06	±4.65E-08
IINm2p5VAIN	-1.00E-06	1.00E-06	±4.15E-08
BIPOLAROFFSET	-2.00E+01	2.00E+01	±1.65E-01
BIPOLARGAINERROR	-6.00E+01	6.00E+01	±2.43E-01
INT(p)NONmLIN		2.00E+00	±1.79E-01
INT(m)NONmLIN	-2.00E+00		±1.34E-01

An ISO 9001:2008 and DSCC Certified Company



SEL Characterization Report
10-xxx 100429 R1.0

Radiation Assured Devices
5017 N. 30th Street
Colorado Springs, CO 80919
(719) 531-0800

CODEWIDTH(DNL)LONG	1.00E+00	2.50E+00	±2.04E-01
CODEWIDTH(DNL)SHORT	-5.00E+00	1.00E+00	±9.99E-02
SFDR	8.60E+01		±3.96E+00
THD		-8.60E+01	±4.10E-01
SINAD	7.80E+01		±1.14E-01

Appendix D: CREME96 Orbit Definition Output File

Created by CREME96:HI_UPSET_DRIVER Version 200 on 01-May-10 at 20:37:01
Input Integral LET Spectrum File: GEOSYNC.LET
Created by CREME96:LETSPEC_DRIVER Version 200 on 18-Dec-07 at 22:15:43
ZMIN = 1 ZMAX = 92 LETMIN = 1.00E+00 LETMAX = 1.10E+05 MeV-cm²/g LBINS = 1002
EMINCUT = 1.00E-01 MeV/nuc
TARGET MATERIAL = SILICON
Input File to LETSPEC_DRIVER: GEOSYNC.TFX
Created by CREME96:TRANSPORT_DRIVER Version 200 on 18-Dec-07 at 22:15:41
ZMIN = 1 ZMAX = 92 EMIN = 1.0000E-01 EMAX = 1.0000E+05 MeV/nuc MBINS = 1002
Thickness = 100.0000 mils ALUMINUM
Input File to TRANSPORT_DRIVER: GEOSYNC.FLX
Created by CREME96:FLUX_DRIVER Version 200 on 18-Dec-07 at 22:15:39
ZMIN = 1 ZMAX = 92
IMODE = 0 SOLAR-QUIET MODE: YEAR = 1977.0000
ITRANS = 0 GEOSYNCH/NEAR-EARTH INTERPLANETARY FLUXES